

Non extensive description of pp collisions at high energies

M. Abdel-Aziz^{1,2}, S. Abdel-Razik³ and M. Sirag³

¹ Basic Science Department ,Faculty of Computers and Information Sciences, Ain Shams University, Khalifa El-Maamon St, Cairo-11566, Egypt

² Scientific Computing Center ,Faculty of Computers and Information Sciences, Ain Shams University , Khalifa El-Maamon St,Cairo-11566, Egypt

³ Physics Department, Faculty of Women, Ain Shams University, AsmaaFahmi, Al Golf, Nasr City, Cairo-11566, Egypt

Abstract. Non extensive statistics provide an excellent application in the field of high energy collisions to study the thermal properties of the produced particles. We apply the scaled Tsallis equation to study the entropy parameter as a function of transverse momentum of the produced hadrons. We applied Tsallis-Pareto to study the transverse momentum distribution of produced hadrons (π^\pm , k^\pm , p , \bar{p}) in pp collisions at center of mass energies $\sqrt{s_{NN}} = 62.4$, 200, 900 GeV and 2.7 TeV . The Pareto-Tsallis distribution, leads to an excellent description of data on transverse momentum distribution .The q parameters are almost independent from \sqrt{s} for protons and kaons and distributed around $q = 1.1$ and q is increasing for pions from 1.1 to almost 1.3 at top energy $\sqrt{s} = 2.7 TeV$. The effective temperature, T increases with collisions energy we estimated $T \approx 0.3 GeV$ for pp collisions at 2.7 TeV LHC energy. Different hadrons have different effective temperature such that heavier hadrons have higher freezeout temperature.

Key words:

Transverse momentum distribution, high energy collision, The Pareto-Tsallis distribution, Non extensive statistics, QGP.

1. Introduction

The transverse momenta of secondary identified particles produced in pp collisions is very important. Since QCD description of low p_t particles is not available because of non perturbative effects. Phenomenological models has been proposed to solve this problem of description p_t distribution in pp and nucleus-nucleus collisions. For example at low p_t where the spectra is in the form of exponential decay hadron gas model with conventional Boltzmann Gibbs distribution are widely used to describe p_t spectra and multiplicity distribution. For high p_t particles, the exponential BG distribution is not appropriate. Many authors proposed Tsallis distribution as an alternative to describe p_t distribution of produced hadrons in pp collisions in terms of the temperature T and the nonextensive parameters q which measures the degree of equitation of the fireball.

Tsallis distribution with thermodynamic consistent formulation is same as the form of QCD inspired Hagedorn distribution in terms of power n related to q [R. Hagedorn et al, 1983]. The high p_t hadrons coming from initial hard scattering decide the value of n and the low p_t hadrons form the bulk of the spectra decide T . Moreover, to allow the nonextensive parameter q to change with hadron p_t . We use the same ansatz as in [[A] G. G. Barnafoldi et al, 2011]. The ansatz used in the current work is different from the one in [[B] G. G. Barnafoldi et al, 2011] as we will discuss in the rest of this paper. The paper is organized as follows: Sec.2 gives details about the model. In Sec.3 we present the fit to the p_t spectra of different hadrons. In Sec.4 we discuss the model parameters as a function of hadron mass and energy for both positive and negative hadrons. In the last section our concluding remarks are given.

2. Tsallis Distribution

In this section we will introduce a very brief discussion on the Tsallis distribution and discuss the need for a scaled Tsallis distribution that allows for variation of the transverse momentum distribution of the secondary hadrons produced in pp at high energy. In high energy physics a thermodynamic consistent form of Tsallis statistics is needed to describe a system very close to equilibrium [J. Cleymans, 2017].

Let's introduce the standard form of particle number N , the energy E and the pressure P is given by the following expressions:

$$N = gV \int \frac{d^3p}{(2\pi)^3} \left[1 + (q-1) \frac{E - \mu}{T} \right]^{-\frac{q}{q-1}}, \quad (1)$$

$$E = g \int \frac{d^3p}{(2\pi)^3} E \left[1 + (q-1) \frac{E - \mu}{T} \right]^{-\frac{q}{q-1}}, \quad (2)$$

$$P = g \int \frac{d^3p}{(2\pi)^3} \frac{p^2}{3E} \left[1 + (q-1) \frac{E - \mu}{T} \right]^{-\frac{q}{q-1}}, \quad (3)$$

$$\epsilon + P = Ts + \mu n \quad (4)$$

Where n, ϵ , refer to the densities of corresponding quantities. Standard Tsallis equation is shown in Eq.(1). Where T and μ are the temperature and the chemical potential, V is the volume and g is the degeneracy factor. This equation has q independent p_t . The parameter q is the entropy index that measures the deviation of the distribution from thermal one and is related to temperature fluctuations via

$$q - 1 = \frac{\langle T^2 \rangle - \langle T \rangle^2}{\langle T \rangle^2} \quad (5)$$

So q can be a measure of the degree of thermalization in the created QGP medium that is produced in high energy nuclear collisions at RHIC and LHC. The particle number N is related to the pressure and particle density n by the thermodynamic formula

$$N = V \left. \frac{\partial P}{\partial \mu} \right|_T \quad (6)$$

It is worth to mention that, the above formulation does not include radial or elliptic flow. So the function distribution in Eq.(8) has no φ dependence of even radial flow β since these quantities are almost zero in case of pp collisions in this case the temperature parameter T can be interpreted as effective temperature.

In order to introduce the p_t dependence of the q we want to mention that very recent results produced by the recombination models [R. J. Fries et al,2005] reveals that the recombination of constituent quarks at intermediate p_t is essential to describe the elliptic flow parameters v_2 , π/P ratio and nuclear modification factors R_{AA} . This investigation reveals that we can probe this variation as a function of particles transverse momentum distribution. To allow for such dependence we use the following ansatz [[A]G. G. Barnafoldi et al ,2011,[[B]G. G. Barnafoldi et al ,2011]:

$$\alpha \rightarrow \alpha(p_t) = \frac{1}{1-q} - A \log \log(1 + k \cdot p_t) \quad (7)$$

So, now the standard Tsallis equations turn to be

$$\frac{d^2 N}{2\pi dy p_t dp_t} = C m_t \left[1 + \frac{m_t}{\alpha T} \right]^{-\alpha} \quad (8)$$

Here $C = gV/(2\pi)^2$ is the overall constant, with g is the degeneracy and V is the volume. $m_t = \sqrt{m^2 + p_t^2}$ is the transverse mass of the hadrons. In order to fit the experimental data and assess the quality of the fit. We use χ^2 as follows

$$\chi^2 = \sum_{i=0}^{n_{obs}} \frac{(O_{exp}(p_{ti}) - O_{theory}(p_{ti}))^2}{\sigma_i^2} \quad (9)$$

Where $O_{exp}(p_{ti})$, $O_{theory}(p_{ti})$ stand for the measured value of p_t distribution and the corresponding theoretical function evaluated at the same p_t using Eq. (8) and σ_i^2 corresponds to combined statistical and systematic errors and n_{obs} is the number of data points.

3. Results

We apply Eq.(8) to fit the experimental data using χ^2 fit. We use the standard ROOT class TMinuit to perform the χ^2 fit. We start by applying the modified Tsallis distribution Eq.(8) to study transverse momentum distribution $\frac{d^2 N}{2\pi dy p_t dp_t}$ of particles produced in high

energy experiments at relativistic heavy ion collider RHIC at energies 62.4 and 200 GeV and at large hadron collider LHC at energies 900 GeV and 2.7 TeV.

In the current work, We focus on the p_t distribution of π^\pm , k^\pm , p , \bar{p} produced in pp collisions at RHIC and LHC. We use Eq. (8) to fit the p_t distribution and get a systematic studies on how the model parameters and average transverse momentum $\langle p_t \rangle$ change with collisions energies and hadron mass.

First we study RHIC results of pp collisions at center of mass energies $\sqrt{s} = 62.4$ and 200 GeV as measured by PHENIX [A. Adare et al,2011] at mid rapidity $y = 0$.

In fig.1 we use eq. (8) to fit the transverse momentum distribution of π^\pm , k^\pm , p , \bar{p} produced in pp collisions at $\sqrt{s} = 62.4$ GeV as measured by PHENIX Eq.(8). It is clear that the experimental data are well reproduced within the measured transverse momentum $0.140 \leq p_t \leq 3$. In order to investigate the applicability of our model to higher energies used in RHIC, we apply Eq. (8) to the same particles as those in fig. 1 but in pp collisions at different energies $\sqrt{s} = 200$ as measured by PHENIX [A. Adare et al,2011]fig.2.

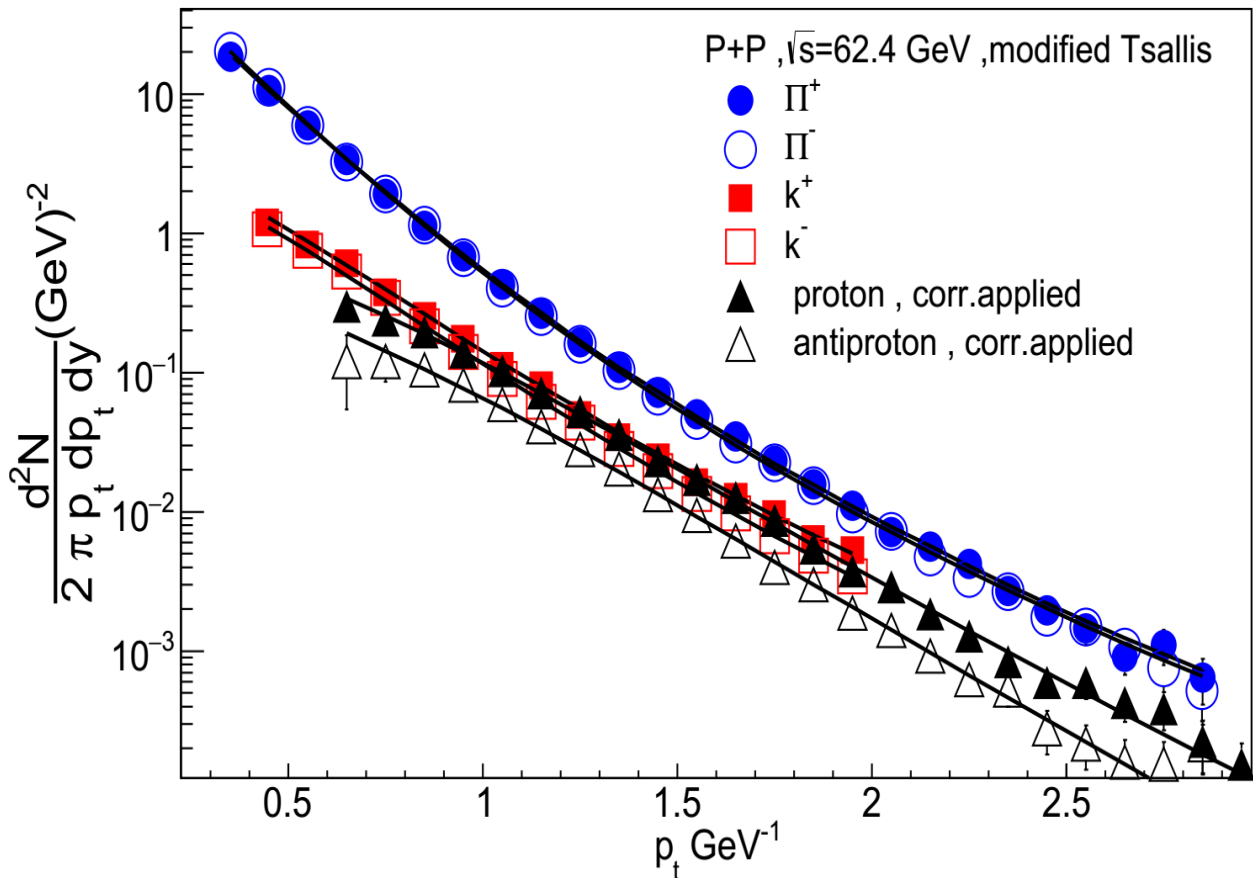


Figure 1: Transverse momentum distribution of π^+ , π^- , k^+ , k^- , proton and antiproton produced in pp collisions as obtained by the PHENIX Collaboration [A. Adare et al,2011] at $\sqrt{s} = 62.4$ GeV at midrapidity. The solid curves are the fits of the data of the modified Tsallis Eq. (8) at midrapidity.

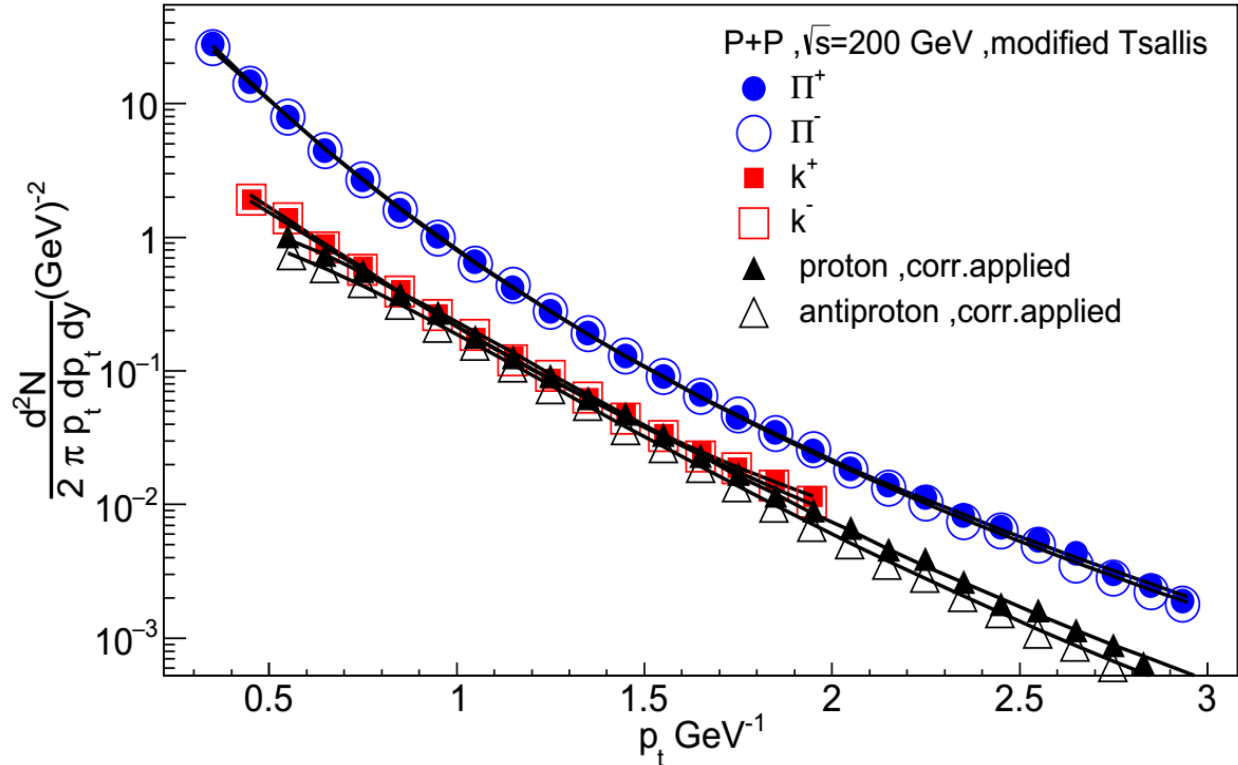


Figure 2: Transverse momentum distribution of π^+ , π^- , k^+ , k^- , proton and antiproton produced in pp collisions as obtained by the PHENIX Collaboration [A. Adare et al,2011] at $\sqrt{s}= 200\text{GeV}$ at mid rapidity. The solid curves are the fits of the data of the modified Tsallis Eq.(8) at mid rapidity.

As shown in fig.(2) both pareto-tsallis model and the experimental data are in excellent agreement within the given p_t range $0.5 \text{ GeV} < p_t < 3.0 \text{ GeV}$.

Both figures clearly indicate that the transverse momentum distribution of π^\pm , k^\pm , p , \bar{p} produced in pp collisions at RHIC at two different energies are well produced.

To explore the applicability of the model to higher energies at LHC, we use the recent data measured by ALICE at LHC for pp collisions at 900 GeV. In Fig.3, we use Eq.(8) to fit the data of identified hadrons produced in pp collisions at 900 GeV in LHC as measured by [K. Aamodt et al, 2011]. We see good agreement between measured values and Eq.(8) for the measured range $0.1 \text{ GeV} < p_t < 2.5 \text{ GeV}$. In fig.4, we show the results of applying Eq.(8) to fit the charged particles distribution $\pi^+ + \pi^-$, $k^+ + k^-$, $p + \bar{p}$. For $\pi^+ + \pi^-$ agreement between model and data is appealing up to $p_t \approx 18 \text{ GeV}$. While for pp and $k^+ + k^-$ the deviation starts to appear at about $p_t \approx 4 \text{ GeV}$. Recently, [G. Wilk and Z. Włodarczyk,2017], [G. Wilk and Z. Włodarczyk,2015], showed that the inclusion of an oscillating factor in the nonextensive parameters can handle the oscillation found in fitting the experimental data for hadrons produced during pp collisions. We will not go into the details of the nature of this oscillation because it is outside the scope of the current work.

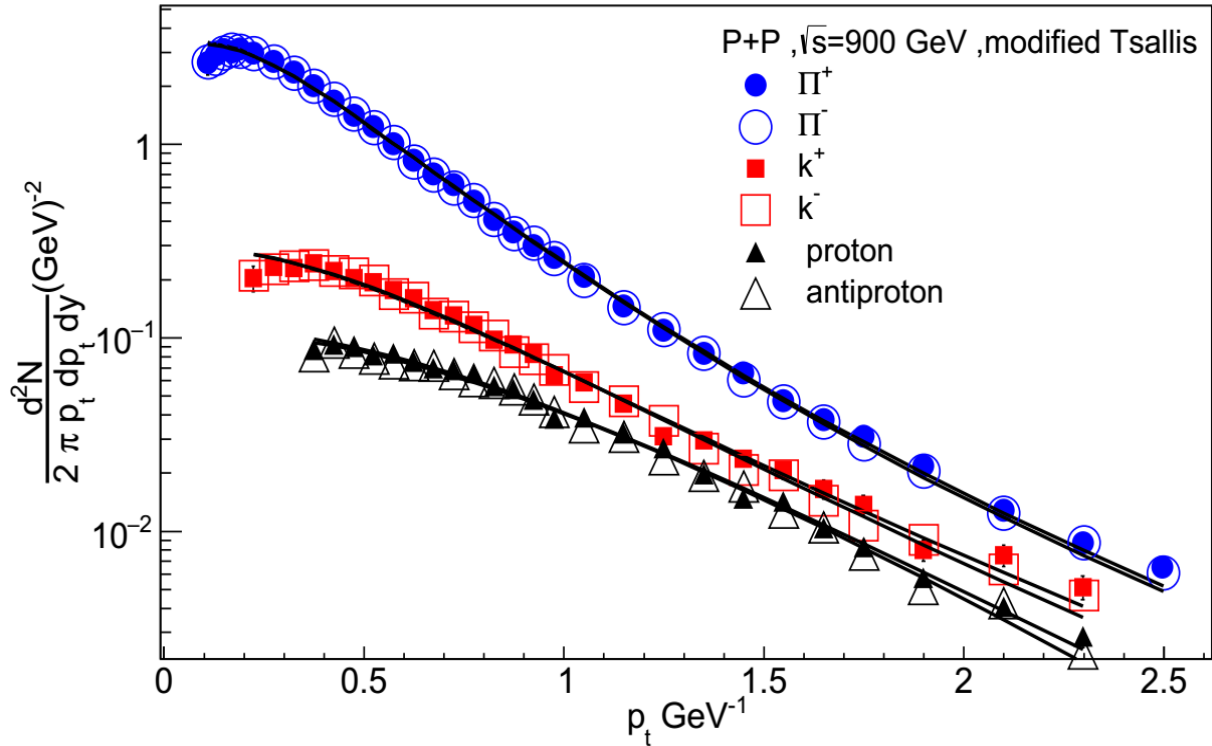


Figure 3: Transverse momentum distribution of π^+ , π^- , k^+ , k^- , proton and antiproton produced in pp collisions as obtained by ALLC Collaboration [K. Aamodt et al, 2011] at $\sqrt{s}=900\text{GeV}$ at midrapidity. The solid curves are the fits of the data of the modified Tsallis Eq.(8) at midrapidity.

4. Model Parameters

In previous section we presented the results of fitting the p_t distribution of different charged hadrons. In this section we will explore the model parameters and their significance and how they vary as a function of collision energy and hadron mass and also comment on the accuracy of our fit procedures. In tables (1, 2, 3, 4) we show the computed parameters in Eq.(8) with the corresponding χ^2/ndf , where ndf is the number of degrees of freedom, for fitting pp data at 62.4, 200, 900 GeV and 2.7 TeV. We notice for every particle in those tables the corresponding χ^2/NDF is less than 1.0 that gives confidence the model performs very well over the given collision energy for every hadron in the tables. In Figs (5,6) we show the extracted values of the nonextensive parameter q from as a function of collision energy for both negative and positive hadrons respectively. The nonextensive parameter q does not show energy dependence within the error bars but for both π^\pm it is clearly q increases with the collision energy from $q = 1.1$ at 62.4 GeV to $q = 1.3$ at 900 GeV.

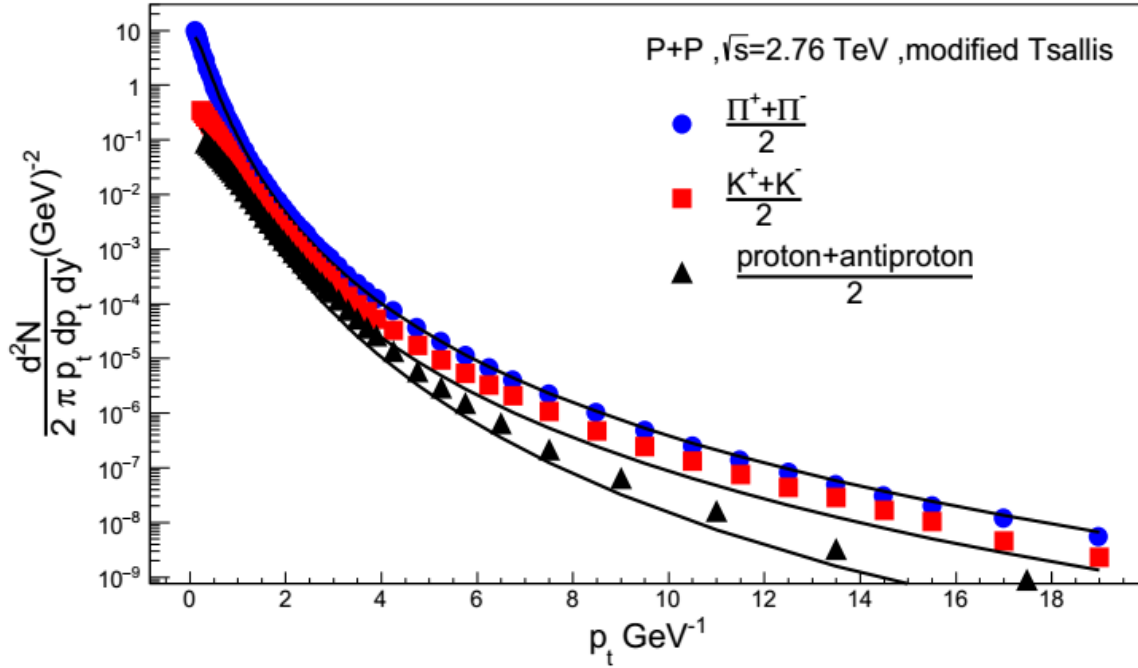


Figure 4: Transverse momentum distribution of π^+ , π^- , k^+ , k^- , proton and antiproton produced in pp collisions as obtained by ALLC Collaboration at $\sqrt{s} = 2.7\text{TeV}$ at midrapidity. The solid curves are the fits of the data of the modified Tsallis Eq.(8) at midrapidity.

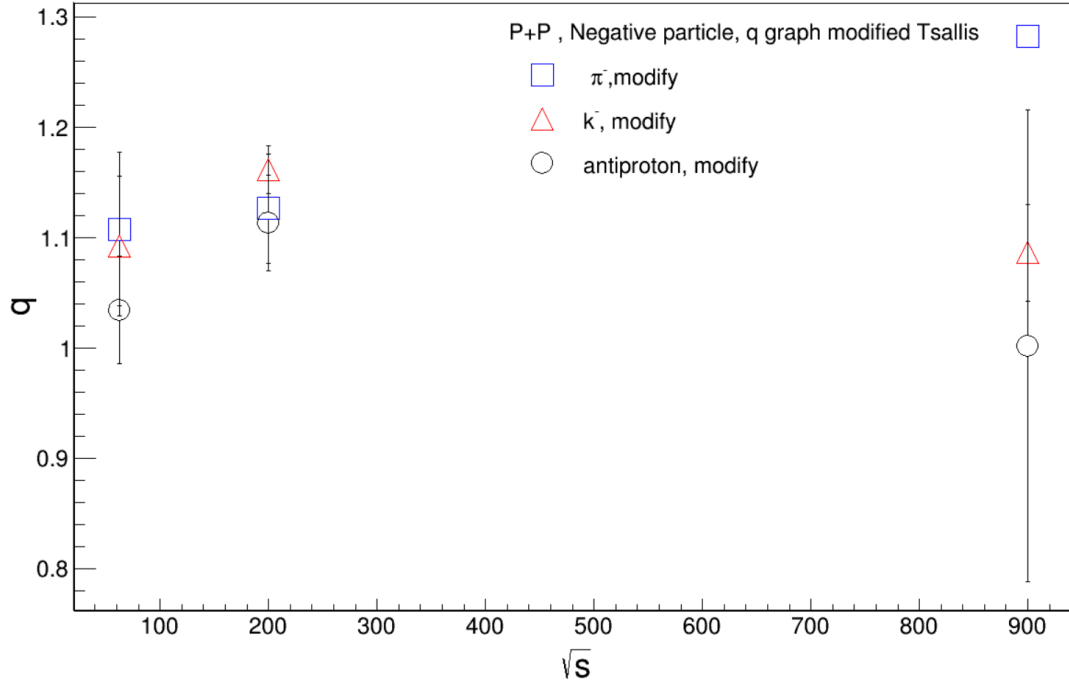


Figure 5: The nonextensive parameter q for -vehadrons versus \sqrt{s}

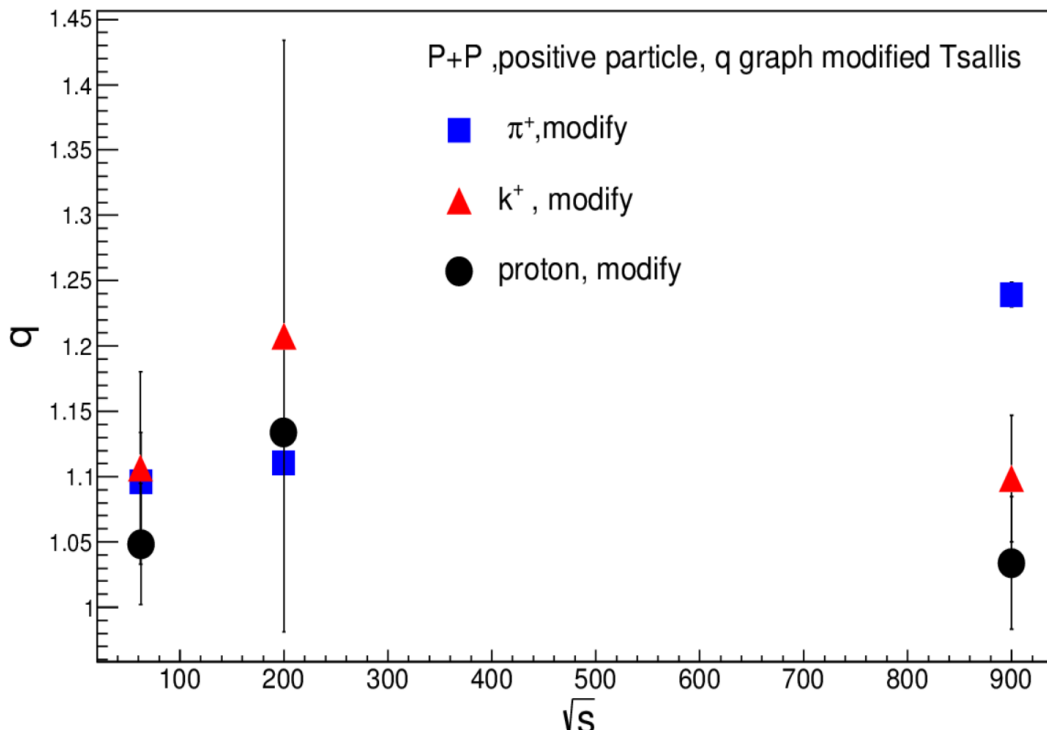


Figure 6: The nonextensive parameter q for +ve hadron versus \sqrt{s}

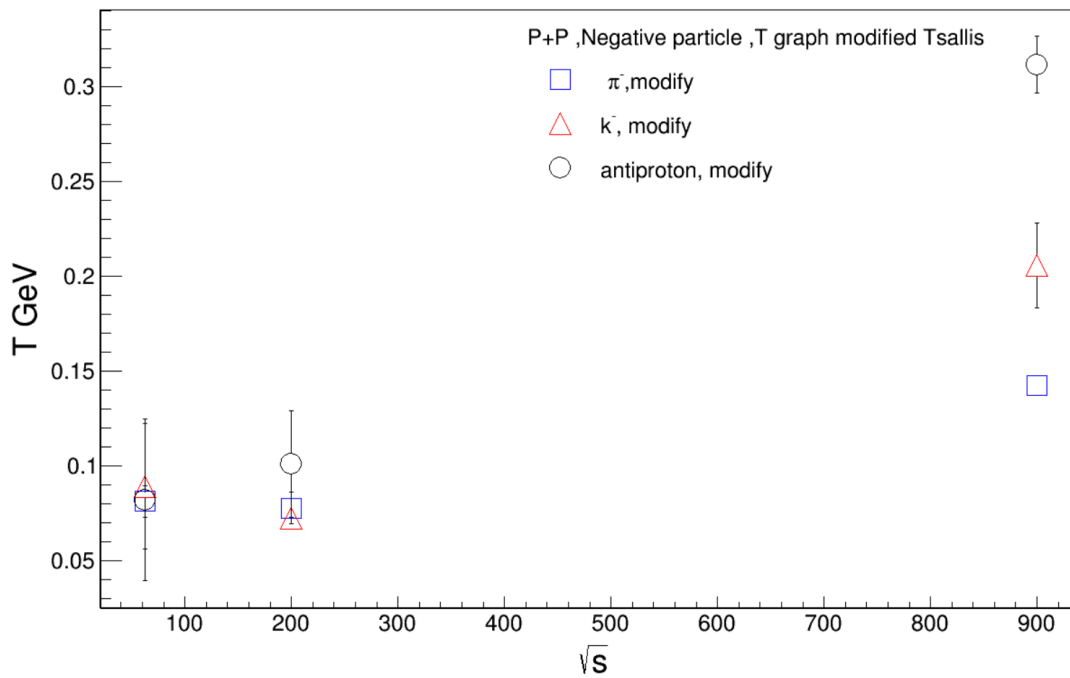


Figure 7: The Temperature parameter T versus \sqrt{s}

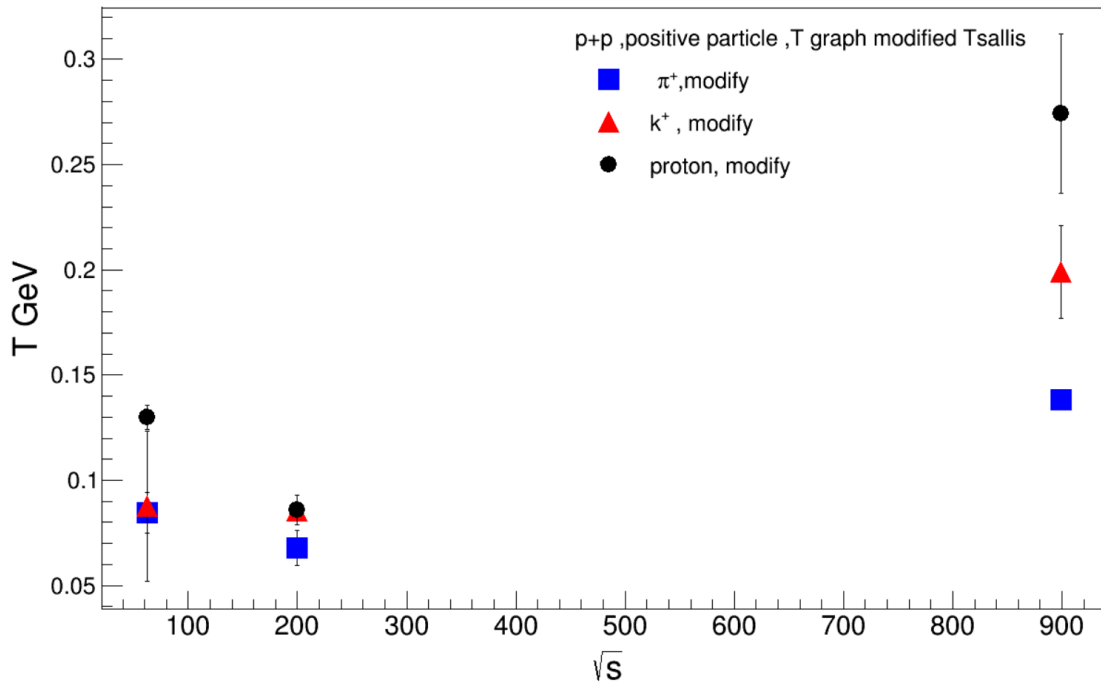


Figure 8: The temperature parameter T versus \sqrt{s}

Now looking to the temperature parameters T in tables (1,2,3,4) and the corresponding figures (9,10,14) we find that T increases with particle mass such that $T_{\pi^\pm} < T_{k^\pm} < T_{p,\bar{p}}$. It clearly indicates that the heavier particles have higher freeze-out temperatures as compared to lighter particles. Also the increases of temperature for p/\bar{p} is more rapid as compared to mesons (π^\pm , k^\pm). The baryons in general freezeout earlier than mesons. This observation goes in-line with an intuitive expectation of mass dependent particle freeze-out or differential freeze-out. This is in agreement with the differential freeze-out scenarios proposed [D. Thaku et al ,2016]. Once all the unknown parameters in Eq.(8) are given as we have shown and discussed. We can compute different observables.

In the current work we will limit ourselves to average transverse momentum $\langle p_t \rangle$ as a function of Hardon mass and energy. In order to do so we define the k^{th} moment of the normalized distribution as

$$\langle p_t^k \rangle = \frac{\int p_t^k \left(1 + \frac{p_t}{\alpha T}\right)^{-\alpha} p_t dp_t dy d\phi}{\int \left(1 + \frac{p_t}{\alpha T}\right)^{-\alpha} p_t dp_t dy d\phi} \quad (10)$$

The ϕ dependence drops out since the distribution is symmetric with respect to ϕ as mention in section 1.

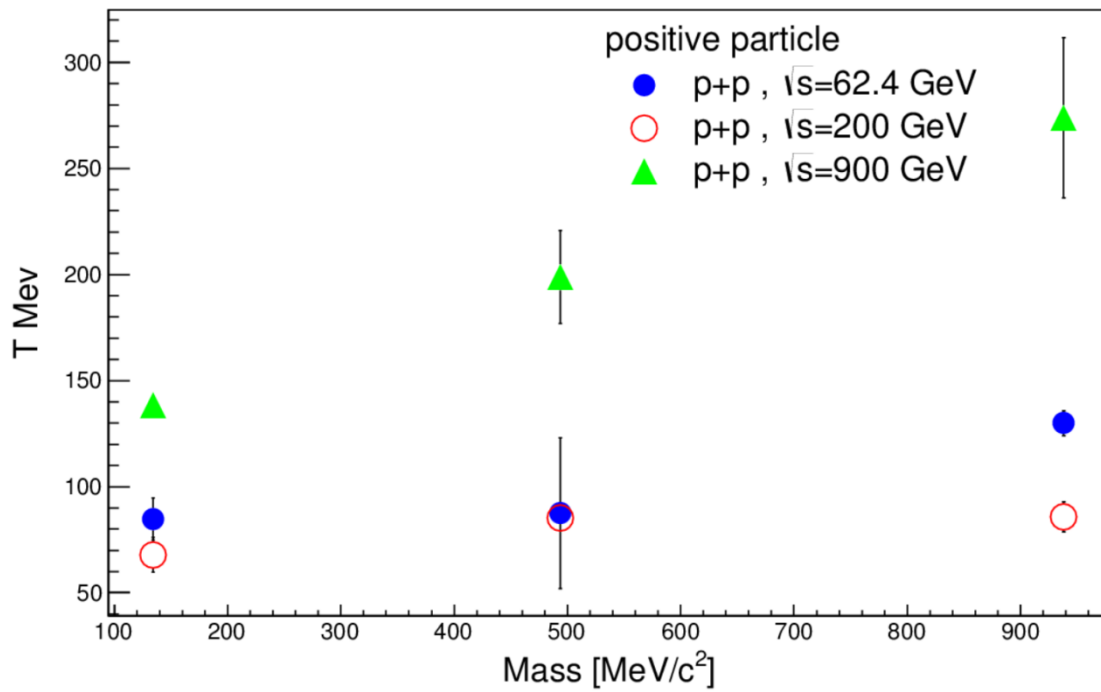


Figure 9: Temperature T of positive hadrons versus their masses.

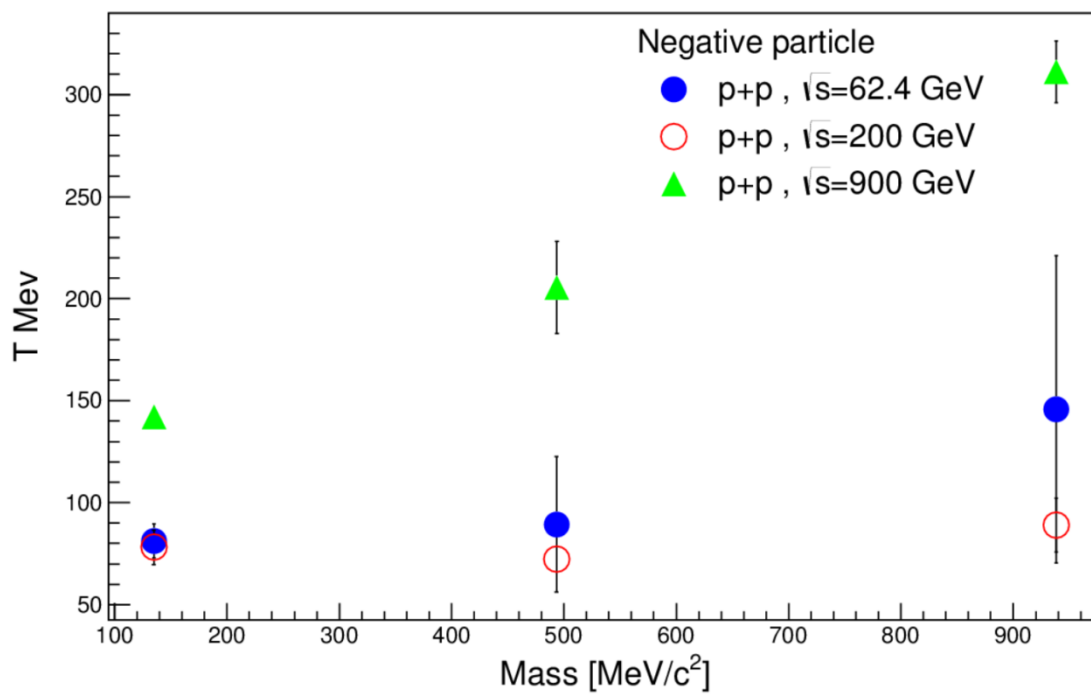


Figure 10: Temperature T of negative hadrons versus their masses.

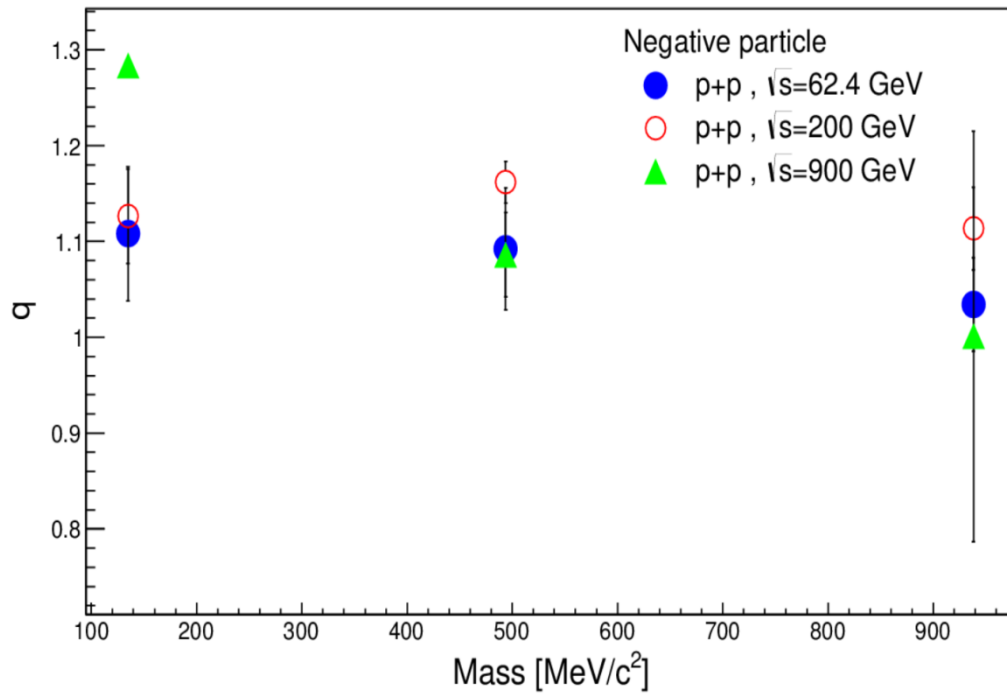


Figure 11: The nonextensive parameter q versus negative hadron mass

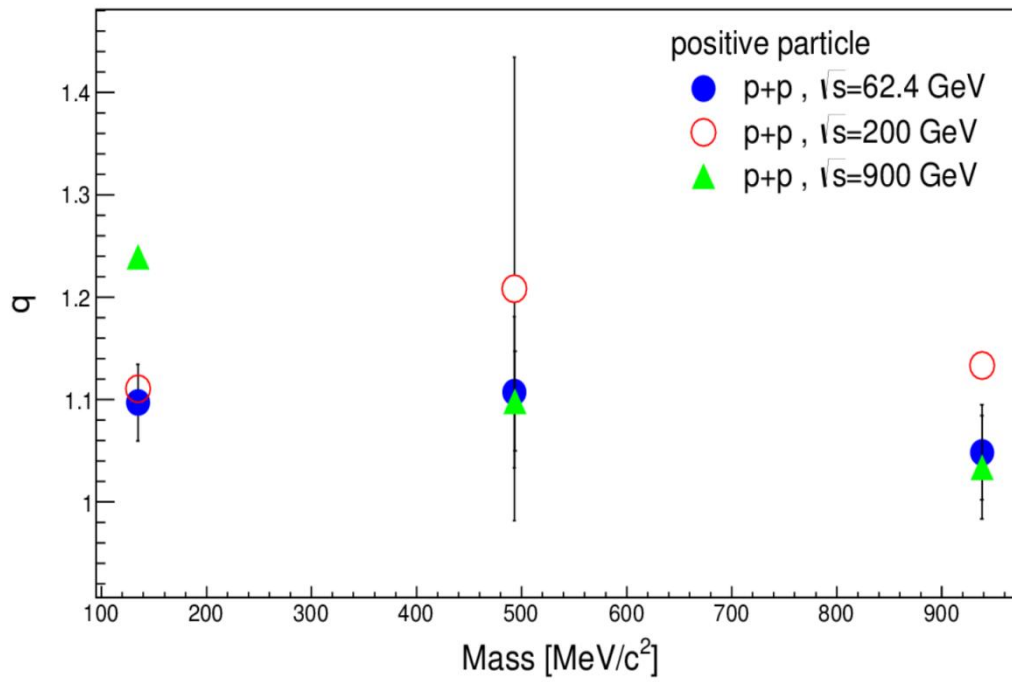


Figure 12: The nonextensive parameter q versus positive hadron mass

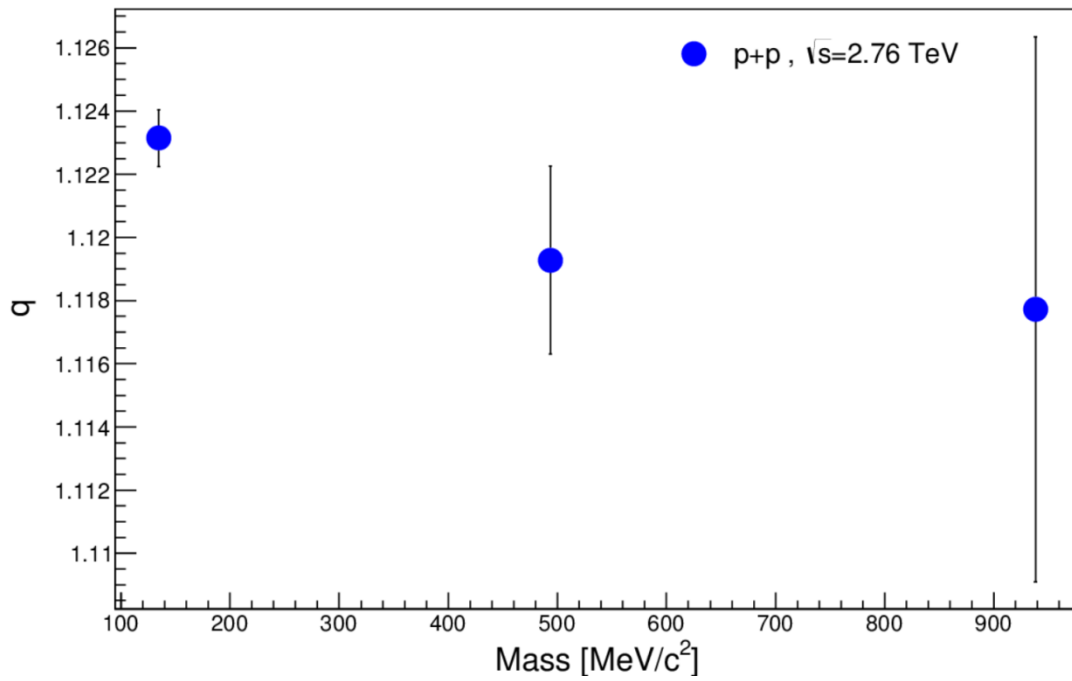


Figure 13: The nonextensive parameter q versus hadron mass

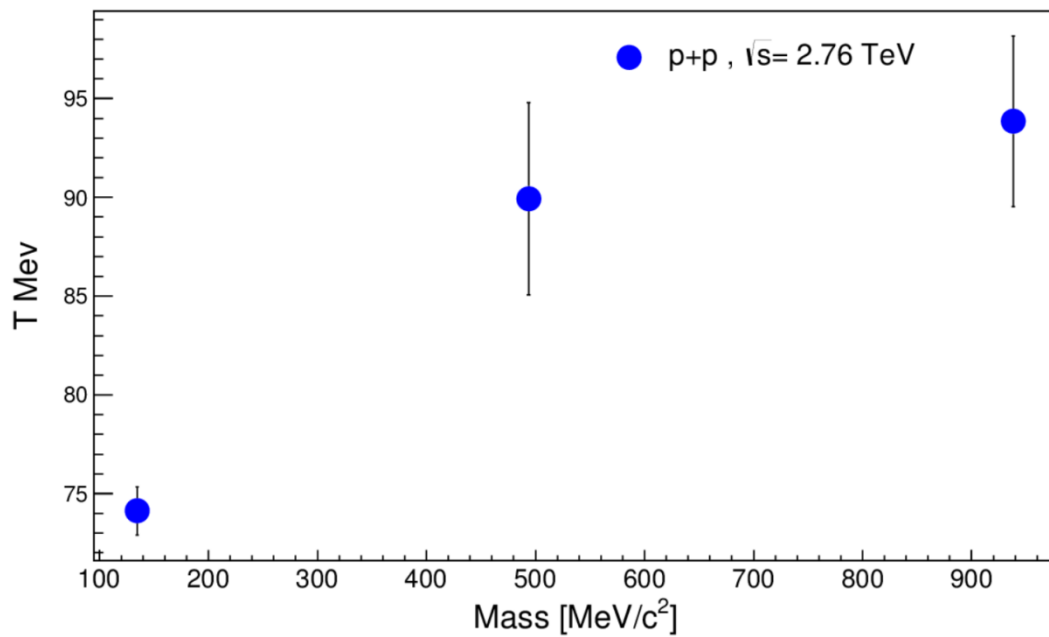


Figure 14: The temperature parameter T versus hadron mass.

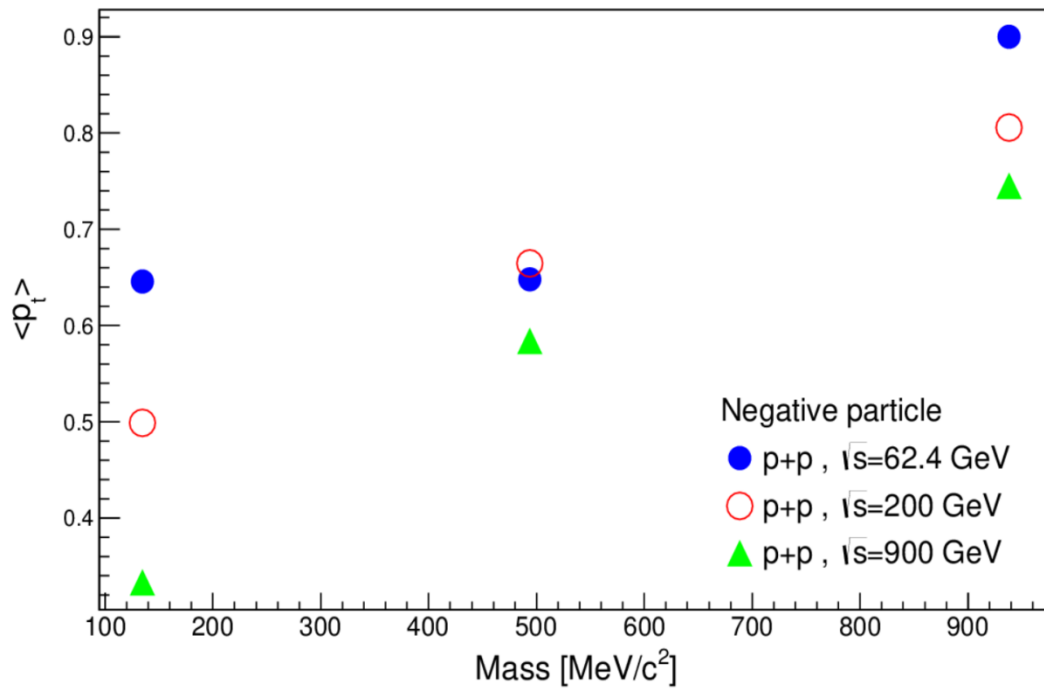


Figure 15: $\langle p_t \rangle$ of negative hadrons versus collisions energy

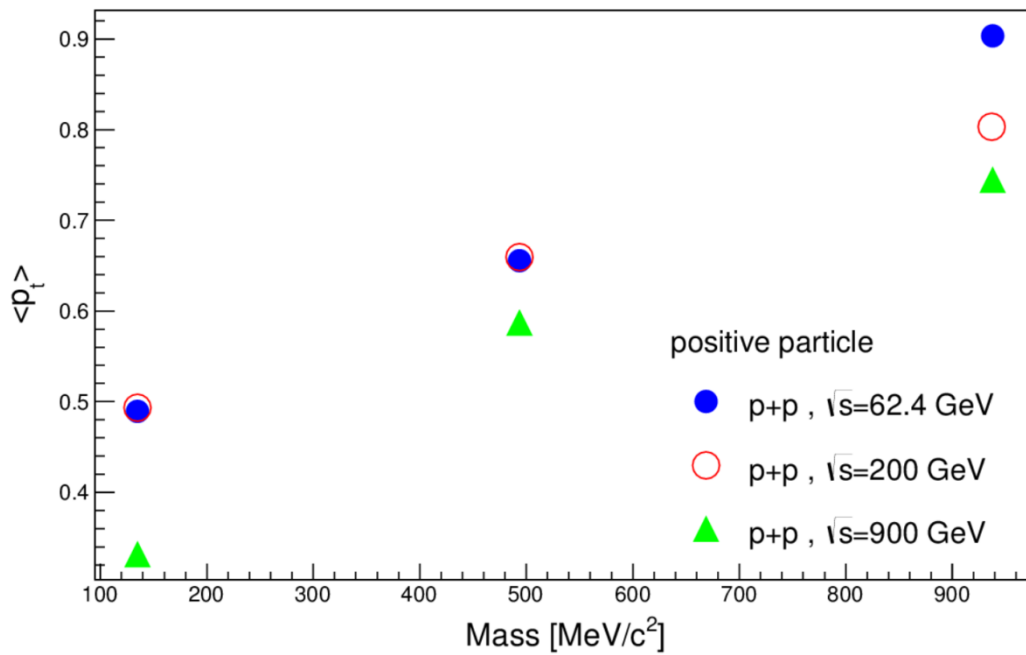


Figure 16: $\langle p_t \rangle$ of positive hadrons versus collisions energy

The first moment $k = 1$ corresponds to $\langle p_t \rangle$ and the second moment $k = 2$ corresponds to $\langle p_t^2 \rangle$ and the variance of the distribution $Var(p_t)$ is given by

$$Var(p_t) = \langle p_t^2 \rangle - \langle p_t \rangle^2$$

In Fig.(15,16) we present the results of our calculations of $\langle p_t \rangle$ as a function of hadron mass using Eq.(10) with $k = 1$. We find that the $\langle p_t \rangle$ increases with increasing hadron mass such that $\langle p_t \rangle_{\pi^\pm} < \langle p_t \rangle_{k^\pm} < \langle p_t \rangle_{p, \bar{p}}$.

5. Discussion and Conclusion

In conclusion, the Pareto-Tsallis distribution, Eq.8 leads to an excellent description of data on transverse momentum distribution. Taken into account couple of approximations that we have taken such that we neglect the chemical potential of hadrons μ and both radial β and elliptic flow velocity v_2 . By comparing results from 62.4 GeV at RHIC up to 2.7 TeV at LHC it has been possible to extract hadron mass and energy dependence of the parameters n , q and T . We have used momentum dependent entropy index n that scales with p_t dependent power ansatz. Parameters T and q were obtained by using the least square method. We investigated the collisions energy \sqrt{s} dependence of the parameter values q and T . The q parameters were found to be almost independent from \sqrt{s} for protons and kaons and distributed around $q = 1.1$ and q is increasing for pions from 1.1 to almost 1.3 at top energy $\sqrt{s} = 2.7$ TeV. Using the scaling Tsallis-Pareto ansatz, the effective temperature, T increases with collisions energy.

62.4 GeV PHENIX					
particle	T	q	K	A	χ^2/ndf
π^+	0.0846252 ± 0.00986138	1.09606 ± 0.0375843	0.0243774 ± 0.562622	1.00253 ± 6.17546	0.02524104
π^-	0.0812931 ± 0.00832641	1.10778 ± 0.0699158	0.00243036 ± 0.237994	1.00414 ± 5.79771	0.03234616
k^+	0.0875774 ± 0.0355324	1.10644 ± 0.0736864	0.0153147 ± 0.637946	1.03075 ± 7.87473	0.0345318666
k^-	0.0892701 ± 0.0331675	1.09250 ± 0.0634979	0.0537477 ± 2.76598	1.01748 ± 8.96576	0.0185472
p	0.129970 ± 0.00589840	1.04847 ± 0.0464307	0.00492518 ± 2.85060	1.00008 ± 6.41729	0.0281819615
\bar{p}	0.145847 ± 0.0753218	1.03437 ± 0.0488596	0.0194563 ± 2.88255	1.22986 ± 5.04656	0.0433296153

Table 1: χ^2/NDF and different extracted parameters of Eq.(8) for π^\pm , k^\pm , p and \bar{p} produced in pp collisions as measured by PHENIX [A. Adare et al, 2011] $\sqrt{s_{NN}} = 62.4$ GeV.

200 GeV PHENIX					
particle	T	q	K	A	χ^2/ndf
π^+	0.0678695 ± 0.00817861	1.11064 ± 0.00697645	3.36626 ± 2.60700	1.00009 ± 8.62072	0.0256206538
π^-	0.0779004 ± 0.00843204	1.12570 ± 0.0493288	0.0100805 ± 0.160082	1.00166 ± 1.88810	0.0285267307
k^+	0.0854086 ± 0.00279072	1.20751 ± 0.226351	0.360469 ± 0.596220	9.99999 ± 6.40843	0.0089581333
k^-	0.0722678 ± 0.00285162	1.16179 ± 0.0215481	0.00100298 ± 0.154996	1.00000 ± 6.42031	0.0322612666
p	0.0858898 ± 0.00698462	1.13330 ± 0.00964241	0.156297 ± 0.0206761	9.96340 ± 6.45932	0.0533696969
\bar{p}	0.0890633 ± 0.0131642	1.11349 ± 0.0432267	0.0911787 ± 0.264148	6.51280 ± 6.23151	0.0331421212

Table 2: χ^2/NDF and different extracted parameters of Eq.(8) for π^\pm , k^\pm , p and \bar{p} produced in pp collisions as measured by PHENIX [A. Adare et al, 2011] $\sqrt{s_{NN}} = 200$ GeV.

900 GeV LHC					
particle	T	q	K	A	χ^2/ndf
π^+	0.138230 ± 0.00146616	1.23934 ± 0.00941634	0.001 ± 2.62331	1.95096 ± 0.131717	0.2679753125
π^-	0.141800 ± 0.00146408	1.28270 ± 0.00516747	0.001 ± 2.66860	2.35196 ± 0.141445	0.2966096875
k^+	0.198814 ± 0.0219545	1.09856 ± 0.0484162	0.0544865 ± 2.13119	1.00114 ± 6.59155	0.1322776923
k^-	0.205488 ± 0.0225403	1.08618 ± 0.0438780	0.0474702 ± 2.16696	1.00000 ± 6.39829	0.1080511538
P	0.273892 ± 0.0377640	1.03395 ± 0.0505776	0.131847 ± 2.05474	9.99930 ± 6.36347	0.0610578260
\bar{p}	0.311274 ± 0.0150977	1.00100 ± 0.214201	0.00100162 ± 2.48665	1.21121 ± 6.98288	0.0672960869

Table 3: χ^2/NDF and different extracted parameters of Eq.(8) for π^\pm , k^\pm , p and \bar{p} produced in pp collisions as measured by PHENIX [K. Aamodt et al, 2011] $\sqrt{s_{NN}}=900$ GeV.

2.7 TeV LHC					
particles	T	q	K	A	χ^2/NDF
$\frac{\langle \pi^+ + \pi^- \rangle}{2}$	0.740918 ± 0.00122361	1.12312 ± 0.000904546	3.49998 ± 2.25268	1.00000 ± 0.0756364	0.582008412
$\frac{\langle k^- + k^+ \rangle}{2}$	0.899373 ± 0.00486970	1.11928 ± 0.00297296	3.41565 ± 2.41247	1.00349 ± 7.71303	0.025813859
$\frac{\langle p + \bar{p} \rangle}{2}$	0.936463 ± 0.00431326	1.11773 ± 0.00862584	$0.00691535 \pm 0.00920205$	1.00000 ± 0.587674	0.074848958

Table 4: Fit parameter for pp collisions at 2.7TeV LHC

Since increasing the collisions energy may result in a higher energy density and higher temperature. We estimated $T \approx 0.3$ GeV for pp collisions at 2.7 TeV LHC energy. further studies is needed to scan low energy pp collisions and get full picture on how the measured parameters depend on energy and hadronic masses and also take into account both radial and elliptic flow of identified hadrons.

6. Reference

A. Adare et al. [PHENIX Collaboration], Phys. Rev. C 83, 064903.

doi:10.1103/PhysRevC.83.064903 [arXiv:1102.0753 [nucl-ex]], **(2011)**.

D. Thakur, S. Tripathy, P. Garg, R. Sahoo and J. Cleymans, Acta Phys. Polon. Supp. 9, 329.

doi:10.5506/APhysPolBSupp.9.329 [arXiv:1603.04971 [hep-ph]], **(2016)**.

D. Thakur, S. Tripathy, P. Garg, R. Sahoo and J. Cleymans, Adv. High Energy Phys. 2016,

4149352 .doi:10.1155/2016/4149352 [arXiv:1601.05223 [hep-ph]],**(2016)**.

[A]G. G. Barnafoldi, K. Urmosy and T. S. Biro, J. Phys. Conf. Ser. 270, 012008.

doi:10.1088/1742-6596/270/1/012008, **(2011)**.

[B]G. G. Barnafoldi, T. S. Biro, K. Urmosy and G. Kalmar, Tsallis-Pareto-like distributions in hadron- hadron collisions, in Gribov-80,eds.Y.LDokshitzer,P.Levai and J.Nyiri .

doi:10.1142/9789814350198-0034(world Scientific,**2011**).

G. Wilk and Z. Wlodarczyk, [arXiv:1701.06401 [hep-ph]],**(2017)**.

G. Wilk and Z. Wlodarczyk, Entropy 17, 384 .doi:10.3390/e17010384 [arXiv:1501.02608

[cond-mat.stat-mech]], **(2015)**.

J. Cleymans, J. Phys. Conf. Ser. 779, no. 1, 012079 .doi:10.1088/1742-6596/779/1/012079

[arXiv:1609.02289 [hep-ph]], **(2017)**.

K. Aamodt et al. [ALICE Collaboration], Eur. Phys. J. C 71, 1655 doi:10.1140/epjc/s10052-

011-1655-9 [arXiv:1101.4110 [hep-ex]] , **(2011)**.

R. Hagedorn, Riv. NuovoCim. 6N10, 1. doi:10.1007/BF02740917, **(1983)**.

R. J. Fries, S. A. Bass and B. Muller, Phys. Rev. Lett. 94, 122301

doi:10.1103/PhysRevLett.94.122301 [nucl-th/0407102], **(2005)**.

وصف تصادم بروتون-بروتون الغير قابل للاتساع عند الطاقات العالية

محمد حسن عبد العزيز^{1,2} و شيماء محمد عبد الرازق³ و منال سراج³

١ - استاذ مساعد بقسم العلوم الاساسيه - كلية الحاسبات والمعلومات - جامعه عين شمس

٢ - رئيس مركز الحساب العلمي - كلية الحاسبات والمعلومات - جامعه عين شمس

٣ - قسم الفيزياء - كلية البنات - جامعه عين شمس

الملخص العربي

الاحصائيات الغير قابلة للاتساع تعطي تطبيق ممتاز في مجال تصادمات الطاقات العالية لدراسة الخواص الحرارية للجسيمات

النتيجة من التصادمات . في هذا البحث طبقنا معادلة (تسالييس) المعاييرة لدراسة معامل الانتروبي كدالة في كمية التحرك

المستعرضه للهادرونات الناتجة. طبقنا توزيع تسالييس-باريتو لدراسة كمية التحرك المستعرضه

الهادرونات ($\bar{p}, p, k^{\pm}, \pi^{\pm}$) في تصادمات البروتون- بروتون عند طاقه مركز الكتلة ($\sqrt{s_{NN}} = 62.4, 200, 900 \text{ GeV}$) و

عند 2.7 TeV . توزيع تسالييس -باريتو تقودنا الى وصف دقيق للبيانات في توزيع كمية التحرك المستعرضه. المعامل (q)

دائما غير معتمد علي \sqrt{s} للبروتونات (p) وكايونات (k) ويتراوح حول ($q=1.1$) ويزداد هذا المعامل للبايونات (π) من

1.1 الي حوالي 1.3 عند اقصى قيمة للطاقة $\sqrt{s} = 2.7 \text{ TeV}$. درجة الحرارة المؤثرة T تزداد مع طاقه التصادمات

حوالي $T = 0.3 \text{ GeV}$ لتصادم بروتون-بروتون عند طاقة المصادم الهبيديروني الكبير 2.7 TeV . الهادرونات المختلفة لها

درجات حرارة مؤثرة مختلفة مثلا الهادرونات الثقيلة لها اعلي درجة حرارة تجمد خارجي .